Corrosion Resistance Behaviour of recycled AlSi10Mg alloy: Surface Morphology and Acoustic Emission Investigation

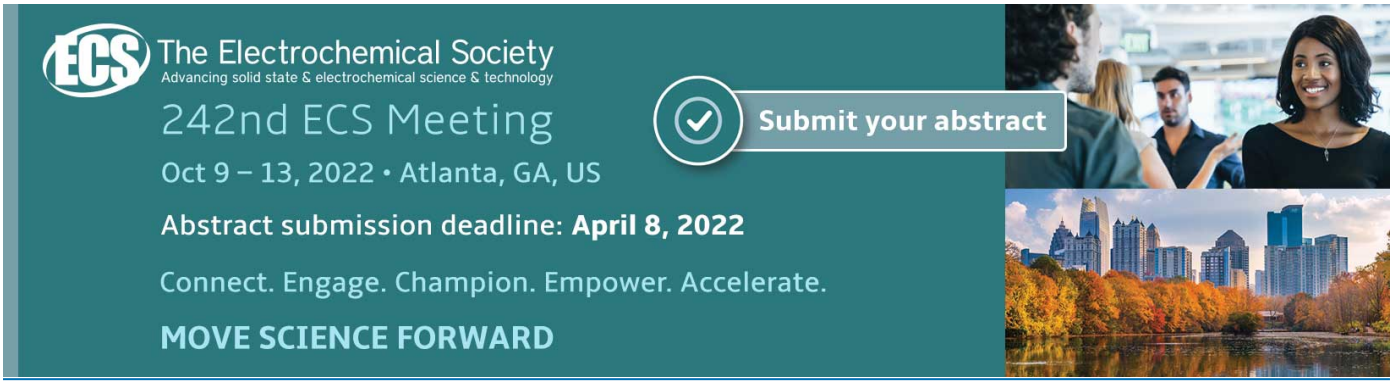

Corrosion Resistance Behaviour of recycled AlSi10Mg alloy: Surface Morphology and Acoustic Emission Investigation

C Barile[a], C Casavola[a], PK Vimalathithan[a] and G Renna[a]

[a] Dipartimento di Meccanica, Matematica e Management, Politecnico di Bari, Via Orabona 4, 70126 – Bari, Italy

claudia.barile@poliba.it

Abstract. The corrosion resistance behaviour of recycled AlSi10Mg alloy prepared using Selective Laser Melting (SLM) process is investigated. The specimens are exposed to salt solution attack (5% NaCl) atomized in uniform droplets, inside a controlled Salt Spray Test (SST) chamber for 1000 h. The surface morphology of the specimens exposed to different predefined exposure times (0 h, 6 h, 48 h, 168 h, 480 h and 1000 h) are investigated under Scanning Electron Microscope (SEM). The SEM micrographs shows the salient features of the corrosion attack such as the formation both of pits and corrosion products on samples surface in different exposure times in the SST chamber. Similarly, the Acoustic Emission (AE) signals generated during the corrosion process are recorded for the different exposure times. The AE waveforms are studied using advanced waveform processing techniques. The waveforms, in their time-frequency domain, provide detailed information on the characteristic features of the acoustic source. The different AE sources have been characterized from the time-frequency analysis of the waveforms.

1. Introduction

Additive Manufacturing (AM) techniques theoretically eliminates the necessity of chip formation or the requirement of lubrication during the manufacturing process. This enables the conservation of stock material and avoids any toxic chemical wastage as a result of the lubrication. However, the unused and un-melted stock materials during these processes are rarely recycled or reused. Particularly, in laser-based AM processes such as Selective Laser Sintering (SLS) or Selective Laser Melting (SLM), some of the feed stocks are deposited over the heated bed and exposed to the regions of proximity to the high-energy laser source [1-4]. This results in the change in the particle size, density, and morphology, which may affect the reusage of these feed materials [5, 6]. Nonetheless, some research works in the past have shown the successful reuse of the recycled feed materials in the SLM process [7, 8].

In this research work, the corrosion resistance behaviour of the recycled AlSi10Mg powder in the test specimens manufactured using the SLM process is studied. The test specimens prepared from the recycled feed material are exposed to SST chamber for simulating the environment-corrosion process for up to 1000 h. Acoustic Emission (AE) technique is used for monitoring the corrosion progressing the material exposed to the salt solution attack. The stress waves generated from a material due to the irreversible deformation occurring within the material propagates at an ultrasonic velocity. Recording

and analysing these stress waves using a piezoelectric transducer forms the basic principle of AE technique [9].

The acoustic waves generated from different sources of corrosion progression such as spallation, formation of corrosion products, and pit formation may differ from each other in terms of their amplitude and frequency content. This study aims in understanding the corrosion behaviour of the AlSi10Mg recycled powder manufactured using SLM process in terms of the time-frequency characteristics of the acoustic waves generated from the test specimens.

2. Experimental Procedure

2.1. Materials and Methods

Recycled AlSi10Mg powder is used as the feed material for preparing dog-bone shaped test specimens using SLM process in RenAM 500 M system. A high-power Nd:YAG laser source of 400 W is traced over the deposited AlSi10Mg powder on the preheated bed to prepare the specimens. The recoater is traced along the Y-axis laser scanned along the X-axis to produce a layer thickness of 20 µm. The test specimens are stress relieved by keeping them in an ambient temperature of 300 °C for about 2 h before air-cooling [10]. The schematic of the test specimen is presented in Figure 1.

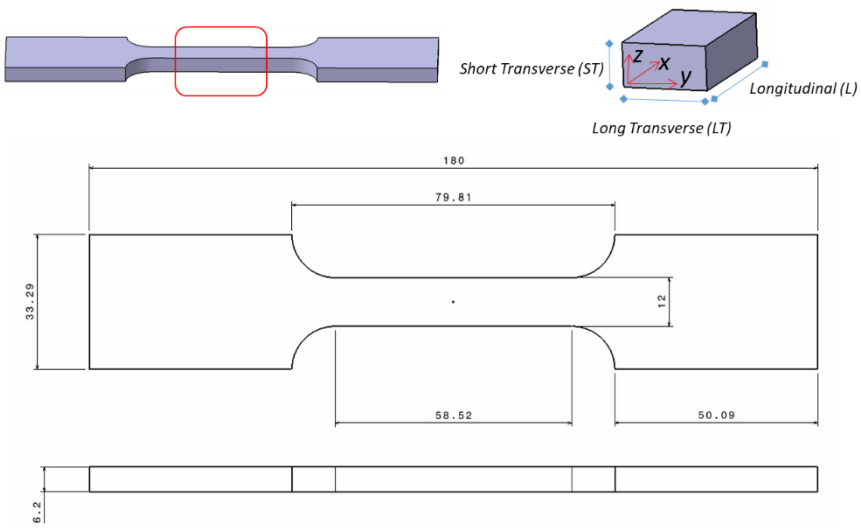

Figure 1. Schematic of test specimen exposed to the SST chamber.

The prepared specimens are placed in a SST chamber (Weiss Technik SC-KWT 450) to simulate the corrosion environment, at temperature of 35 °C. The test is carried out according to the ASTM B117 standard by exposing the test specimens to a 5% NaCl micrometric salt spray with a humidifier temperature and pressure of 48 °C and 0.98 bar, respectively. The exposure times are chosen according to DIN EN ISO 9227 standards: 2, 6, 24, 48, 96, 168, 240, 480, 720 and 1000 hours. After each exposure time, the specimen is taken out, cleaned and then air dried for further analysis. Particularly, the loss mass, density, and surface roughness were evaluated. The mass loss was determined by reweighing and subtracting the panel mass after exposure from its original mass, analogously to the procedure of [11]. The sample weights were evaluated by an analytical balance with 0.1 mg of sensitivity, while the density was calculated using the water displacement method (via the Archimedes method).

The surface roughness of SLS samples post corrosion treatment was measured using a Taylor Hobson Surtronic 25 portable profilometer with a cut-off length of 0.8 mm and a measurement length of 8 mm. Particularly, Ra and Rt roughness parameters were evaluated. Ra is the Roughness Average value that represents the arithmetic average of the absolute values of the roughness profile ordinates, while Rt is Roughness Total height value that indicates the maximum peak to valley height within the

evaluation length. The roughness reported was the average of five values scanned from different areas on the coating surface.

Surface morphologies analysis is performed on the Long Transverse-Longitudinal section (LT-L plane) of the test specimens under Zeiss EVO-MA10 scanning electron microscope (SEM).

For recording the AE generation during the exposure of the specimens to the SST chamber, a piezoelectric sensor with a ceramic core, specially designed for harsh environment is used. The sensor ISR 15 is mounted on the specimens inside the SST chamber. A thin layer of silicone grease is smeared to the transducing surface of the sensor to improve the acoustic coupling. The acoustic waves above a detection threshold of 25 dB are recorded, and pre-amplified by 40 dB using a 2/4/6 AE pre-amplifier. The waves are recorded at a sampling rate of 1 MHz.

2.2. Processing of Acoustic Emission Waves

The recorded acoustic waves are studied in their time-frequency domain using Continuous Wavelet Transform (CWT). Analytical Morlet wavelet with a symmetry parameter of 3, with 3 octaves and 32 voices per octave is used. This wavelet is from a family of analytical wavelets, whose Fourier transform vanishes at negative frequencies. The analytical wavelets are most suitable for CWT, particularly for the group of nonstationary waves such as acoustic waves.

3. Results and Discussions

3.1. Corrosion Behaviour

Salt spray tests were performed in order to understand the corrosion behaviour of the SLS specimen made from recycled AlSi10Mg powder. Corrosion progression was assessed by mass loss and surface roughness measurements, microscopical examination and Acoustic Emissions (AE).

Figure 2 illustrates the ratio between the mass loss due to the corrosive attack and the sample surface exposed to the aggressive environment (mg/cm^2 in Figure 2a), and density values of the specimen during salt spray tests (Figure 2b). It should be observed that the mass loss of the sample was low and almost constant up to 24 h, after this exposure time the trend of mass loss was linearly-decreasing with increasing exposure time (Figure 2a). This decreasing mass loss is related with a weight gains of sample due to an important progressive formation of corrosion products from this time on. It is interesting to note that sign inversion of mass loss (from loss to mass gains) occurs between 24 and 48h of exposure time. As can be observed, following 48 h the mass gain was about 78% after 168 h and 98% after 1000 h.

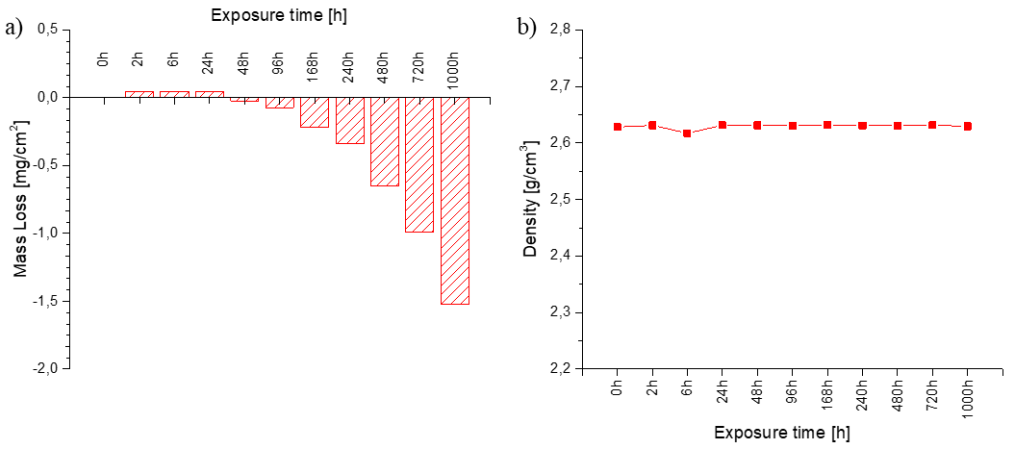

Figure 2. Analysis of the effect of exposure to a controlled corrosive environment of the SLS specimen made from recycled AlSi10Mg powder: a) mass loss (mg/cm^2) and b) density value (g/cm^3) as function of exposure time (h)

Therefore, SLM sample fabricated using recycled powder is characterized by a low surface defectiveness during the first 24 h, exhibiting a corrosion rate almost constant; however, following this exposure time the sample displayed a decrease in corrosion rate as exposure time increased. Besides, by looking at Figure 2b it is worthwhile to note that density values of the samples remained constant with increasing exposure time in SST chamber, indicating that no occurrences are significantly interconnected to the formations and/or changes of open and closed porosity, which could lead to a reduction in physical properties.

Figure 3 shows the Ra and Rt surface roughness of sample as a function of the exposure time in SST chamber. The graph revealed that the Ra and Rt surface roughness values fluctuate slightly with the increasing exposure time. This behaviour is likely due to some simple considerations related to the corrosion phenomenon. During the accelerated aging treatment there is a concomitance of two mechanisms. One, there may be the formation of new micro-porosities (pitting) emerging on the surface as well as an increase in existing ones; on the other hand, the formation of corrosion products. In agreement with literature, the pits on the surface, for the longer exposure times, may also be partially filling by means of material products, whose morphological characteristics depend largely on the corrosive atmosphere that generated them [12, 13], leading to a slight decrease in the Rt roughness.

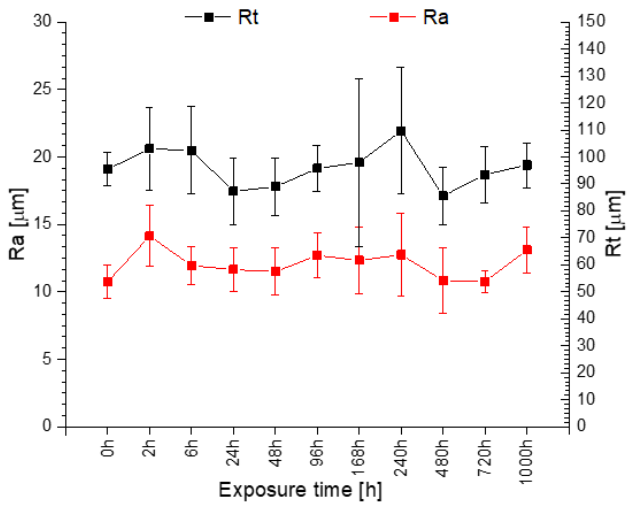

Figure 3. Ra (Roughness Average value) and b) Rt (Roughness Total height value) with respect to exposure time interval to salt spray test.

A careful analysis of the morphological features of the SLM specimen exposed to different duration of the exposure time are depicted in Figure 4. As can be observed, the surface morphology of the as-received SLM sample (before aging - 0 h) was characterized by rough texture resulted mainly from partially melted powder adhering to the surface (balling phenomena). In agreement with literature [6-14], the surface of the sample subjected to SST were characterized by local corrosion: usually manifested by random formation of pits. Specifically, randomly shaped and round pits of small-sizes and shallow could be observed on the surfaces during the first 48 h (see the high-resolution SEM images in Figure 4b and 4c). The corrosion progressed along with exposure time, and simultaneous pits formation on the surface of the samples and refilling of the same by corrosion products occurred. Particularly, it was observed that, following the 48 h of exposure time, the samples surfaces were mainly characterized by corrosion products. After 480 h the surface appears to be more covered by corrosion products with different sizes and morphology. At the end of tests (1000 h), high magnification analysis indicated that the corrosion pits were substantially enlarged and became slightly more marked, inside which it places the corrosion products (Figure 4f). Therefore, morphological analysis using SEM confirmed the remarks of the mass loss results and surface roughness measures.

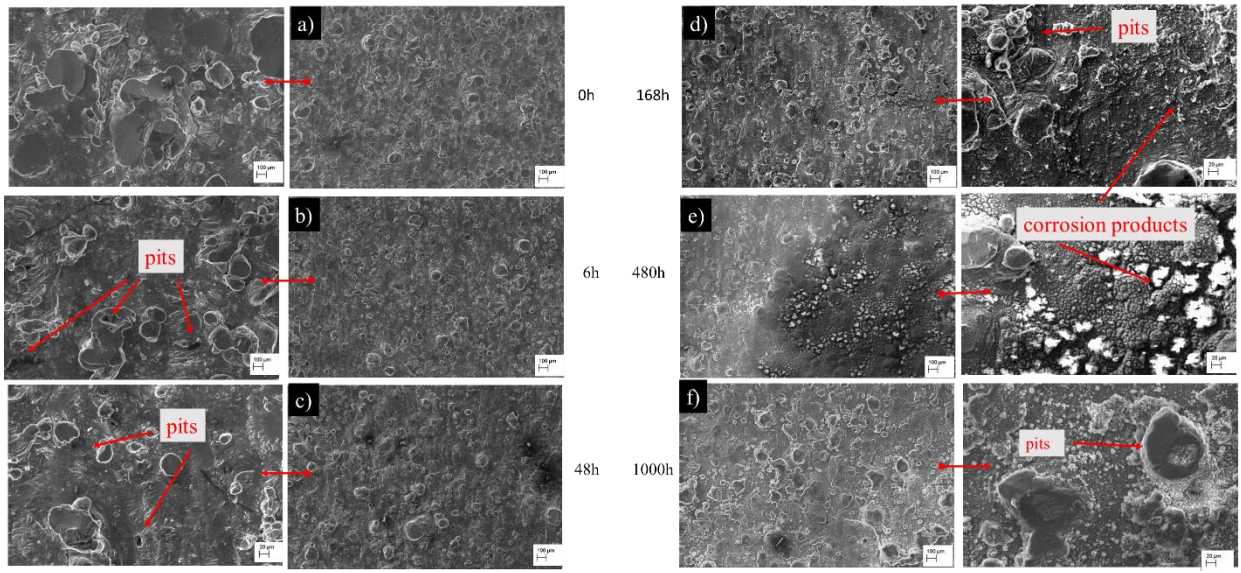

Figure 4. Secondary SEM images of sintered specimen surfaces following 0, 6, 48, 168, 480 and 1000 h of salt spray tests.

3.2. Acoustic Emission Results

Acoustic waves generated during the progression of the corrosion in the AlSi10Mg test specimens are discussed in this section. From the morphological analysis in Section 3.1, it is evident that the corrosion products and pits formed at different exposure times. The formation of these pits and the corrosion products lead to the emission of stress waves, which is propagated through the specimen at different frequencies. The velocities of these waves and the mode of propagation also differs based on their sources. Therefore, differences in their time-frequency characteristics can be observed.

The acoustic waves generated from the different exposure times are analysed in their time-frequency domain. First, during the initial stages of corrosion (between 0 to 6 h), two specific group of acoustic waves are being observed. The time-frequency characteristics of the representative waves from these groups are analysed using CWT results and are presented in Figures 5a and 5b. The first wave in Figure 5a has a frequency centred around 275 kHz to 300 kHz but it has a very short duration. Besides, this wave vanishes after 2800 sample duration. The second wave in Figure 5b, however, has a longer duration of about 7500 samples. Besides, the frequency at which the magnitude maximum magnitude observed is very closely localized to 300 kHz and this magnitude reduces as the reverberations can be observed over the duration before vanishing entirely at 7500 samples.

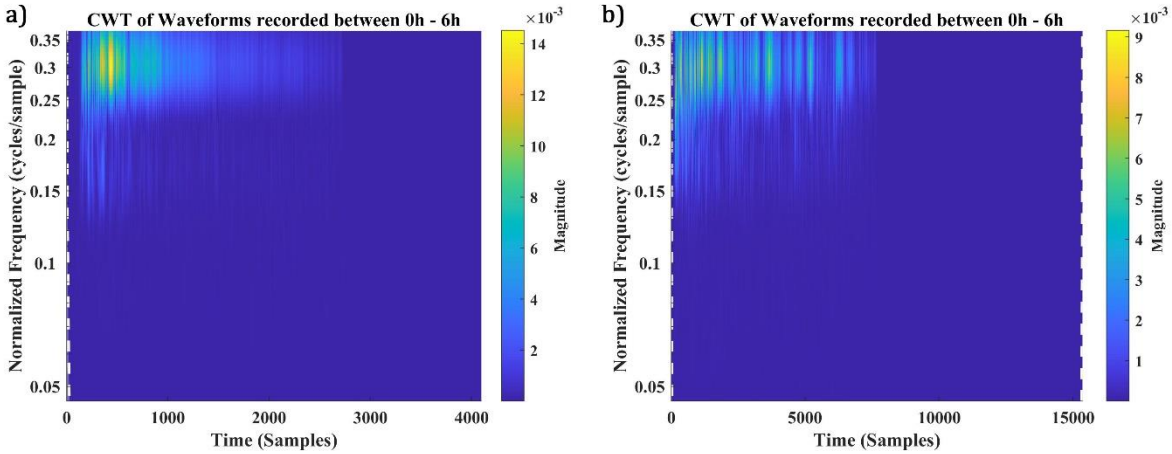

Figure 5. CWT of Waveforms recorded during 0h to 6h duration.

The CWT of the acoustic waves generated during the initial pit formation around 48h exposure time are presented in Figures 6a and 6b. During the pit formation, two more distinct group of acoustic waves are observed. The first acoustic wave in Figure 6a has the frequency with the maximum magnitude around 250 kHz to 300 kHz, similar to the waves from Figure 5, however, it is very short in duration, amounting for about only 700 samples before vanishing. The second group of the acoustic wave in Figure 6b also has the frequency localized around 250 kHz to 300 kHz but some reverberations can be observed up to 1500 samples. First, there is a clear difference between the waveforms during the initial stages of exposure (in Figure 5) and during the pit formation. Although the frequency localization of these waveforms is around 250 kHz to 300 kHz, they vary significantly in terms of their time localization and reverberations.

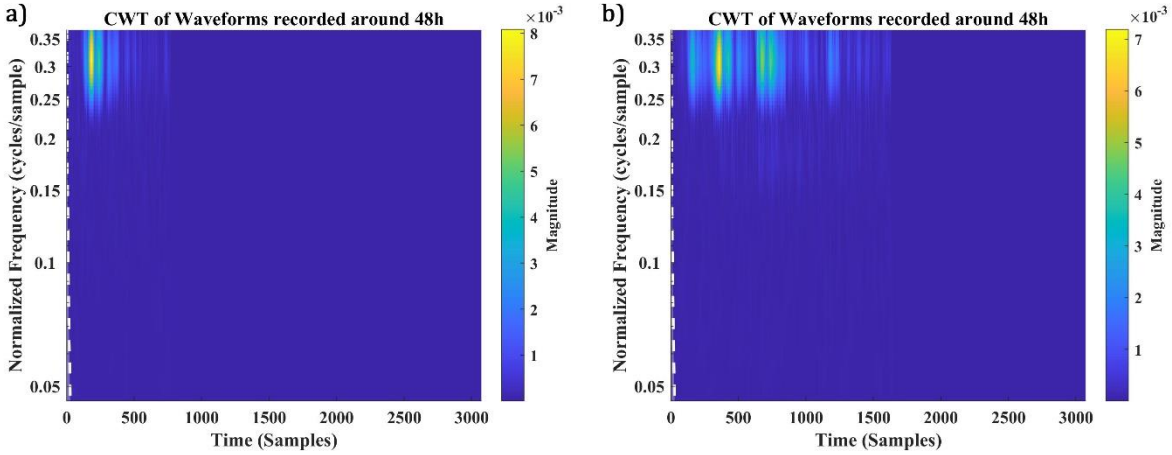

Figure 6. CWT of Waveforms recorded around 48h duration.

Corrosion products have started to form following 48 h and these grow with increasing exposure time, as mentioned in Section 3.1. The CWT of the acoustic waves recorded during 168-480 h exposure time is presented in Figure 7. Interestingly, during this stage, only one group of acoustic waves are recorded. Two examples of this group of acoustic waves are presented respectively in Figures 7a and 7b. The frequency of these acoustic waves is also localized between 250 kHz to 300 kHz but there are two significant differences between these waves and the acoustic waves during the initial stages and pit formation. The frequency localization of these acoustic waves is much shorter in duration and the magnitude of the frequency is much higher. The acoustic waves from the pit formation in Figures 6a and 6b have a maximum magnitude of 7 x 10^{-3}, but the magnitude of waves during the apparent corrosion product formation is between 2.5 x 10^{-2} and 4.5 x 10^{-2}.

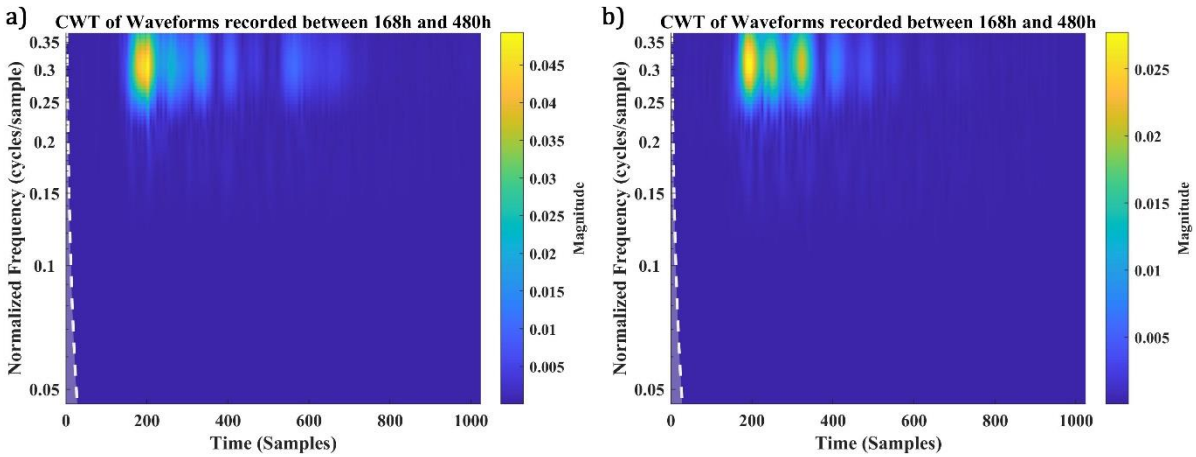

Figure 7. CWT of Waveforms recorded between 168h and 480h duration.

While analysing the acoustic waves at the end of the corrosion exposure, between 720h and 1000 h, formation of corrosion products is observed. Theoretically, the CWT of the acoustic waves observed in this duration must be similar to the acoustic waves in Figure 7. Coincidentally, the frequency localization and the maximum magnitude of the frequency of the acoustic waves generated between 168h and 480h, and 720h and 1000h are the same. The CWT results of the acoustic waves from the end of corrosion exposure is presented in Figure 8. The results show that the maximum magnitude of the frequency around 300 kHz is between 2.2 x 10^{-2} and 3.3 x 10^{-2}. This can lead to the conclusion that there is a significant similarity in the frequency localization and the magnitude of the acoustic waves from the formation of corrosion products between different duration.

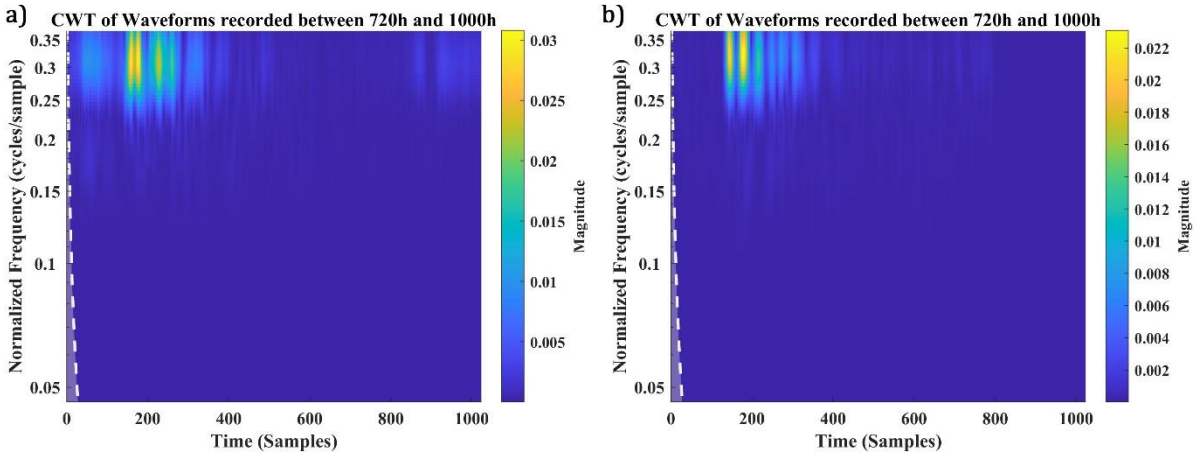

Figure 8. CWT of Waveforms recorded between 720h and 1000h duration.

A general conclusion made from these results about the time-frequency characteristics, the magnitude of the localized frequency and the different sources of the corrosion progression. Pit formation generally generates acoustic waves with low magnitude and longer duration with the frequency localized around 250 kHz and 300 kHz. There are also a lot of reverberations observed in these waves. The formation of corrosion products also generates acoustic waves in the same frequency range but having much larger amplitude and very short duration. Deeper analysis on this time-frequency characteristics can be helpful in identifying the amount of pit and corrosion product formation during the exposure of the recycled AlSi10Mg powder to the controlled corrosive environment.

4. Conclusion

The corrosion behaviour of the AlSi10Mg manufactured using SLM process from the recycled feed material is studied. In general, the corrosion tests performed on the specimens show good corrosion resistance. The surfaces of the samples subjected to SST are characterized by local corrosion. The morphological analysis on the test specimens at different exposure time shows the formation of pits and corrosion products. Particularly, samples are characterized by the low surface defectiveness during the first 24 h, exhibiting a corrosion rate almost constant, following this exposure time the samples displayed a decrease in corrosion rate as exposure time increased due to an important progressive formation of corrosion products from this time on.

Corrosion pits started to form before 48h, and the acoustic waves generated during this same duration have low magnitude, longer duration and frequency localized between 250 kHz and 300 kHz. Formation of other corrosion products occur around 168h to 480h of exposure and also during the final stages of exposure up to 1000 h. The acoustic waves generated during these periods shows a distinct feature of having larger magnitude and higher duration with the frequency around 300 kHz. Therefore, it can be concluded that the corrosion progressions such as formation of pits and corrosion products

can be differentiated using the acoustic emission. The corrosion behaviour, in general, of the recycled AlSi10Mg specimens can be characterized qualitatively using this technique.

References

[1] Asgari H, Baxter C, Hosseinkhani K and Mohammadi M 2017 On microstructure and mechanical properties of additively manufactured AlSi10Mg_200C using recycled powder. *Mater Sci Eng-A* **707** 148-158
[2] Kim DK, Hwang JH, Kim EY, Heo YU, Woo W and Choi SH 2017 Evaluation of the stress-strain relationship of constituent phases in AlSi10Mg alloy produced by selective laser melting using crystal plasticity FEM *J Alloy Compd* **714** 687-697.
[3] Dehoff RR, Tallman C, Duty CE, Peter WH, Yamamoto Y, Chen W and Blue CA 2013 Case study: additive manufacturing of aerospace brackets *Mater Sci Forum* **171(3)**.
[4] Yusuf SM, Hoegden M and Gao N 2020 Effect of sample orientation on the microstructure and microhardness of additively manufactured AlSi10Mg processed by high-pressure torsion *Int J Adv Manuf Tech* **106(9)** 4321-37.
[5] Tang HP, Qian M, Liu N, Zhang XZ, Yang GY and Wang J 2015 Effect of powder reuse times on additive manufacturing of Ti-6Al-4V by selective electron beam melting *Jom* **67(3)** 555-563.
[6] Rafieazad M, Chatterjee A and Nasiri AM 2019 Effects of recycled powder on solidification defects, microstructure, and corrosion properties of DMLS fabricated AlSi10Mg *Jom* **71(9)** 3241-52.
[7] Ardila LC, Garciandia F, González-Díaz JB, Álvarez P, Echeverria A, Petite MM, Deffley R and Ochoa J 2014 Effect of IN718 recycled powder reuse on properties of parts manufactured by means of selective laser melting *Phys Proc* ***56*** 99-107.
[8] Maamoun AH, Elbestawi M, Dosbaeva GK and Veldhuis SC 2018 Thermal post-processing of AlSi10Mg parts produced by Selective Laser Melting using recycled powder *Additive Manuf* **21** 234-247.
[9] Barile C, Casavola C, Pappalettera G and Vimalathithan PK 2020 Application of different acoustic emission descriptors in damage assessment of fiber reinforced plastics: A comprehensive review *Eng Fract Mech* ***235*** 107083.
[10] Barile C, Casavola C, Pappalettera G and Vimalathithan PK 2020 Acoustic emission descriptors for the mechanical behavior of selective laser melted samples: An innovative approach *Mech Mater* **148** 103448.
[11] ASTM International B 117, Standard Practice for Operating Salt Spray (Fog) Apparatus, (2003).
[12] Barile C, Casavola C, Campanelli SL and Renna G 2019. Analysis of corrosion on sintered stainless steel: mechanical and physical aspects *Eng Fail Anal* **95** 273-282.
[13] Liu C, Leyland A, Bi Q and Matthews A 2001 Corrosion resistance of multi-layered plasma-assisted physical vapour deposition TiN and CrN coatings *Surf Coat Tech* **141(2-3)** 164-173.
[14] Revilla RI, Liang J, Godet S and De Graeve I 2016 Local corrosion behavior of additive manufactured AlSiMg alloy assessed by SEM and SKPFM *J Electrochem Soc* **164(2)** C27.